

## Supporting Information

for *Adv. Sci.*, DOI 10.1002/adv.202305405

Facile General Injectable Gelatin/Metal/Tea Polyphenol Double Nanonetworks Remodel Wound Microenvironment and Accelerate Healing

*Xingjie Zan, Dong Yang, Yi Xiao, Yaxin Zhu, Hua Chen, Shulan Ni, Shengwu Zheng, Limeng Zhu\*, Jianliang Shen\* and Xingcai Zhang\**

# Supplementary Materials

## Facile General Injectable Gelatin/Metal/Tea Polyphenol Double Nanonetworks Remodel Wound Microenvironment and Accelerate Healing

Xingjie Zan,<sup>1,2†</sup> Dong Yang,<sup>1,2†</sup> Yi Xiao,<sup>3</sup> Yaxin Zhu,<sup>2</sup> Hua Chen,<sup>4</sup> Shulan Ni,<sup>1,2</sup> Shengwu Zheng,<sup>5</sup> Limeng Zhu,<sup>1,2\*</sup> Jianliang Shen<sup>1\*</sup>, Xingcai Zhang<sup>3\*</sup>

<sup>1</sup> National Engineering Research Center of Ophthalmology and Optometry, Eye Hospital, Wenzhou Medical University, Wenzhou, 325027, China.

<sup>2</sup> Wenzhou Institute, Wenzhou Key Laboratory of Perioperative Medicine, University of Chinese Academy of Sciences, Wenzhou, 325001, China.

<sup>3</sup> School of Engineering and Applied Sciences, Harvard University, Cambridge, Massachusetts, 02138, USA.

<sup>4</sup> Department of Thoracic Surgery, The First Affiliated Hospital of Wenzhou Medical University, Wenzhou, 325003, China.

<sup>5</sup> Wenzhou Celecare Medical Instruments Co., Ltd, Wenzhou, 325000, China.

\* Corresponding authors. Emails: zhulimeng@ucas.ac.cn (Limeng Zhu); shenjl@wiucas.ac.cn (Jianliang Shen); xingcai@seas.harvard.edu (Xingcai Zhang).

† These authors contributed equally to this work and are the first co-authors.

### This PDF file includes:

Figs. S1 to S13  
Table. S1

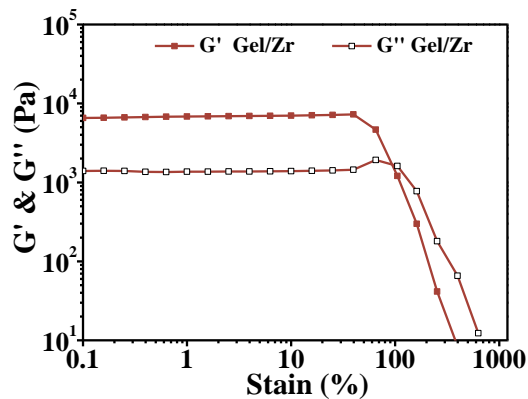


**Fig. S1.** The Strain amplitude sweep test of Gel/Zr hydrogel.

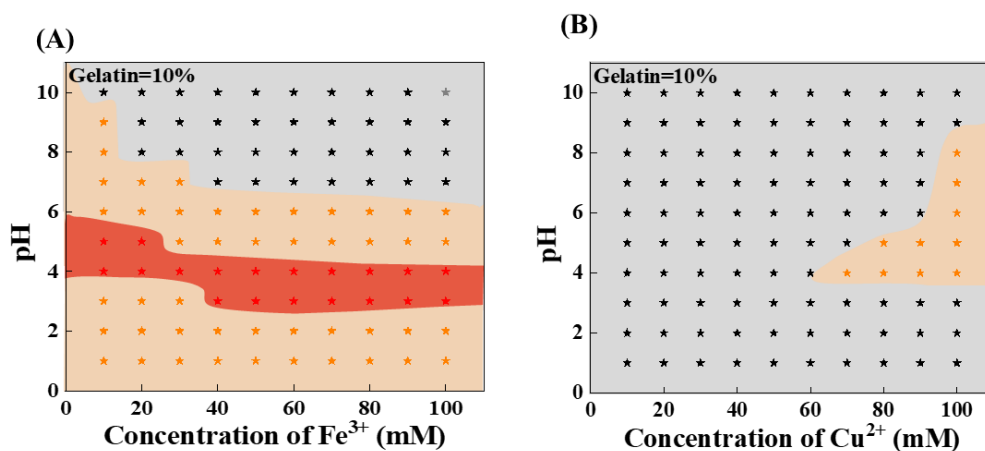


**Fig. S2. Phase diagram of metal ions and Gel.** (A) Gel and  $\text{Fe}^{3+}$  mixtures at different pH. (B) Gel and  $\text{Cu}^{2+}$  mixtures at different pH. According to the different colors of stars, they represent liquid (★), coacervate (★), and hydrogel (★).

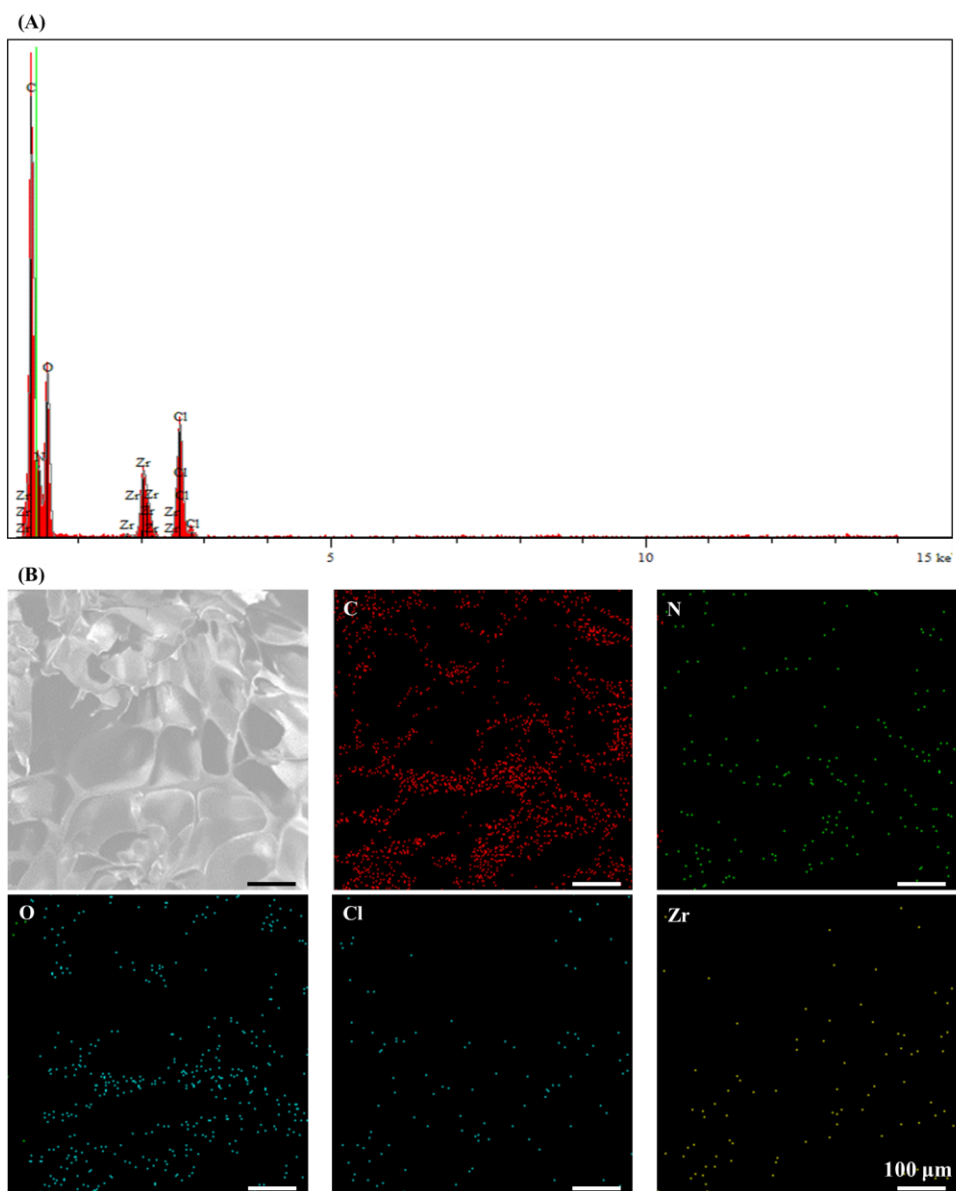


**Fig. S3. Elemental analysis by EDS under SEM.** (A) The EDS spectra of Gel/Zr hydrogel. (B) EDS mapping of Gel/Zr hydrogel.

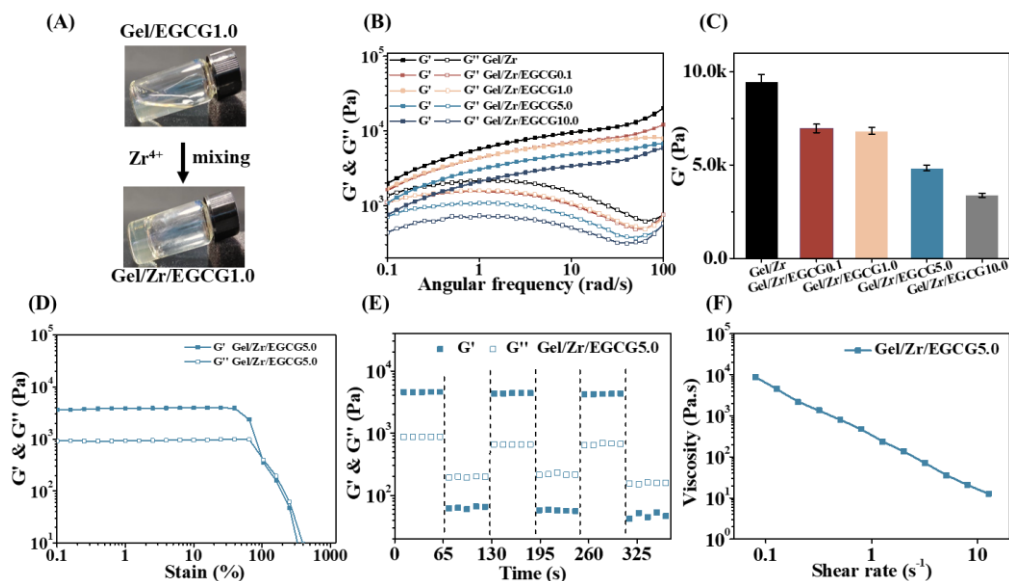


**Fig. S4. Fabrication and Viscoelastic characterization of injectable Gel/Zr/EGCG hydrogels.** (A) The images of Gel/Zr/EGCG1.0 hydrogel. (B) The storage modulus  $G'$  and loss modulus  $G''$  of Gel/Zr/EGCG hydrogels (strain = 1%). (C) The  $G'$  values of Gel/Zr/EGCG hydrogels with different EGCG concentrations (The contents of EGCG in the hydrogel are 0.1, 1.0, 5.0, and 10.0 mg/mL for Gel/Zr/EGCG0.1, Gel/Zr/EGCG1.0, Gel/Zr/EGCG5.0, and Gel/Zr/EGCG10.0, respectively). (D) The Strain amplitude sweep test of Gel/Zr/EGCG5.0 hydrogel. (E) Self-healing properties of Gel/Zr/EGCG5.0 hydrogel under alternating strain from 1% to 400% (frequency = 0.1 Hz). (F) Shear-thinning behaviors of Gel/Zr/EGCG5.0 hydrogel.

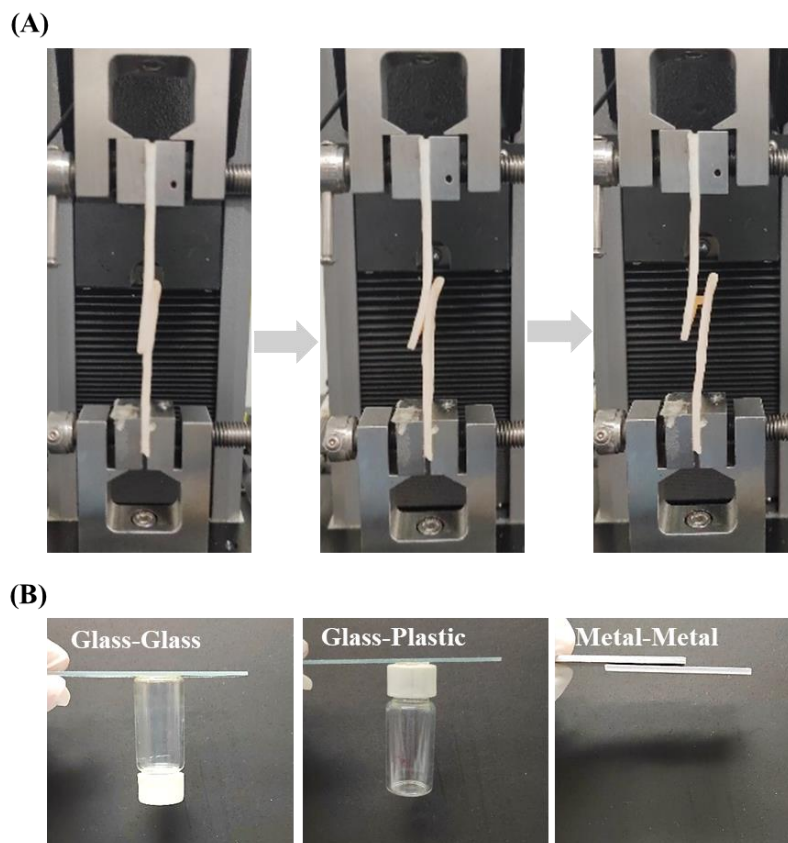


**Fig. S5. Photo of Gel/Zr/EGCG1.0 hydrogel adhesion behavior.** (A) Schematic lap shear test of Gel/Zr/EGCG1.0 hydrogel on pig skin. (B) Pictures of Gel/Zr/EGCG1.0 hydrogel adhesion in different media.

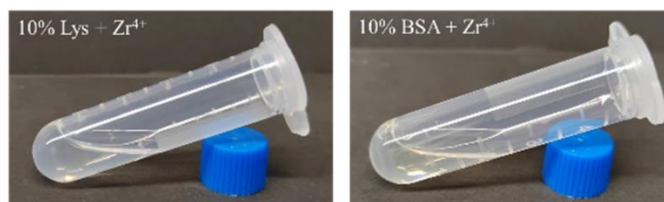


**Fig. S6. Photograph of  $Zr^{4+}$  mixed with lysozyme (Lys) and bovine serum albumin (BSA).**

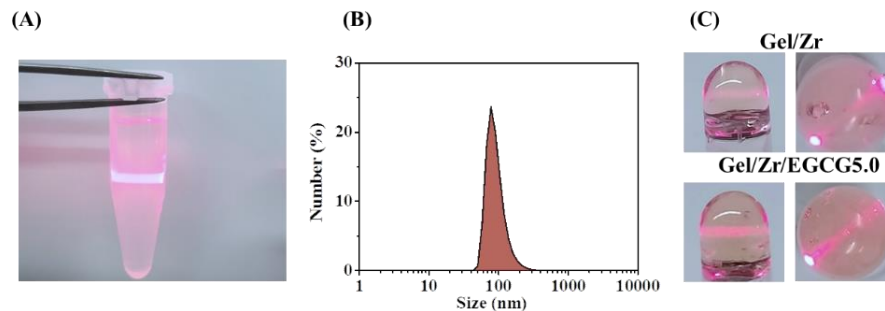


**Fig. S7. Characterization of  $\text{Zr}^{4+}$ /EGCG nanoparticles.** (A) Tyndall effect of nanoparticles formed by coordination of  $\text{Zr}^{4+}$  with EGCG under red laser irradiation. (B) Hydrodynamic size distribution of  $\text{Zr}^{4+}$ /EGCG. (C) Red laser was passed through the Gel/Zr and Gel/Zr/EGCG hydrogels, respectively.

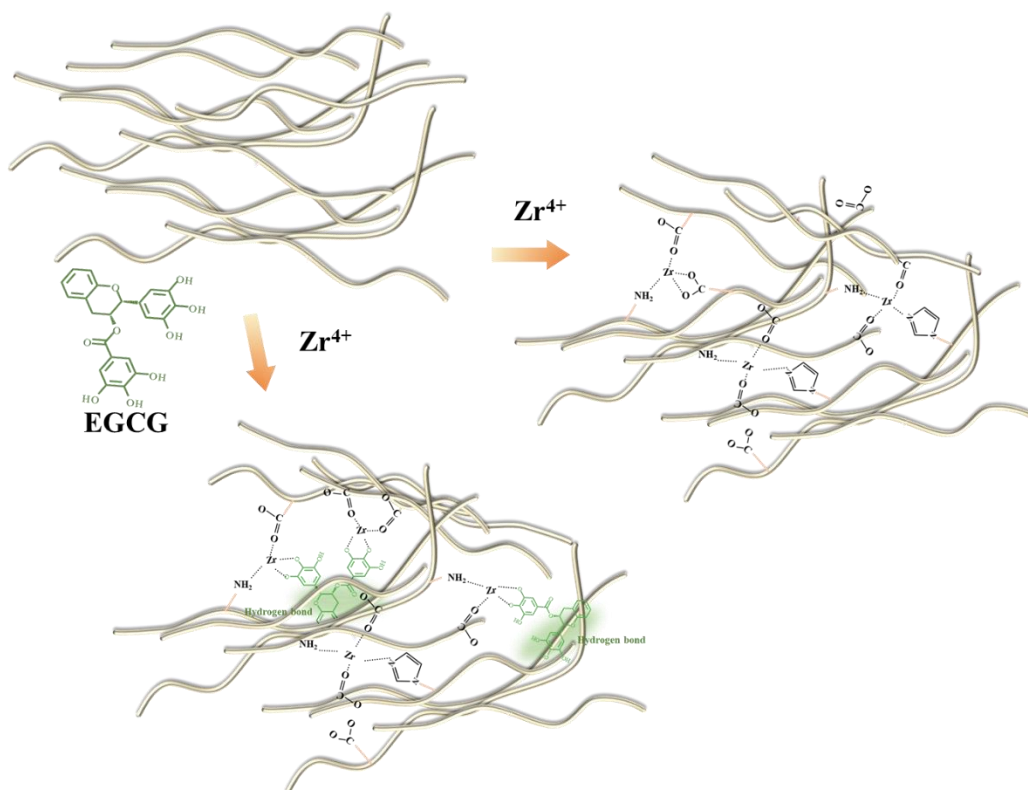


**Fig. S8. Schematic of the coordination chemistry of  $\text{Zr}^{4+}$  with gelatin and EGCG.**

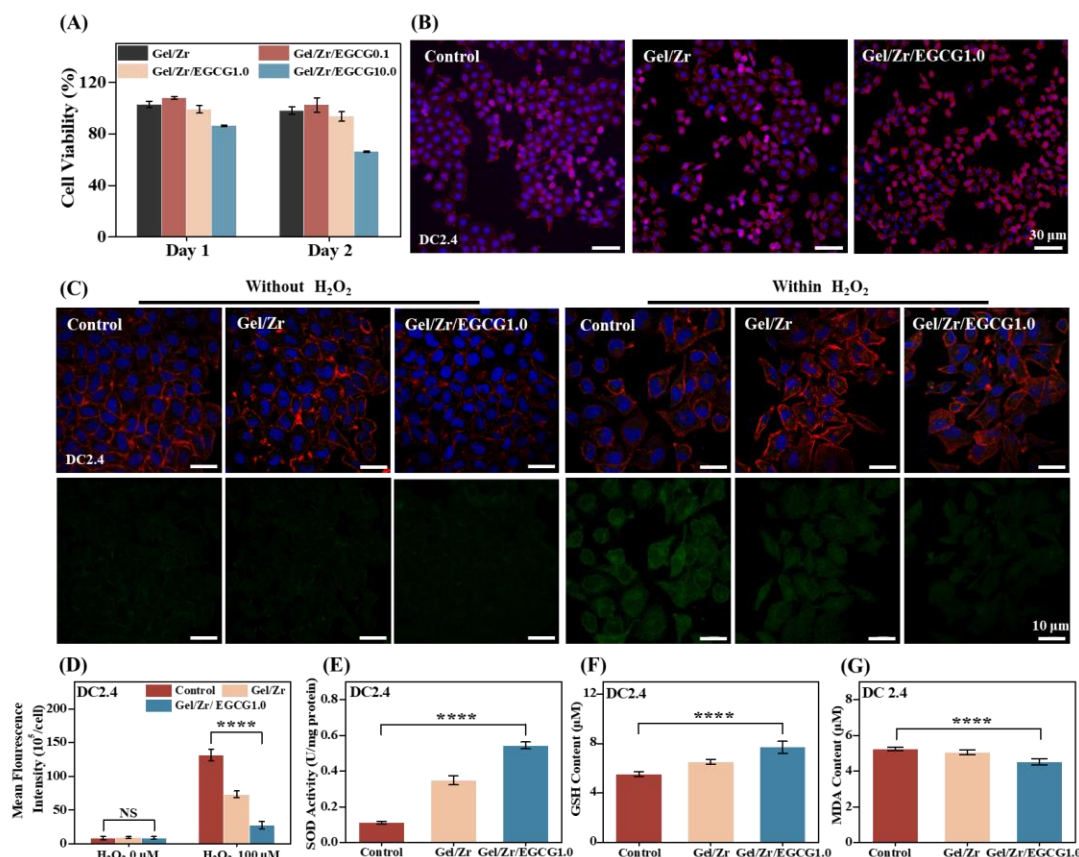


**Fig. S9. *In vitro* biocompatibility and intracellular antioxidant capability of Gel/Zr/EGCG1.0 hydrogel.** (A) The viability of DC2.4 cells cultured in Gel/Zr and Gel/Zr/EGCG hydrogel extracts after one and two days, respectively (n = 5). (B) Fluorescence images of DC2.4 cells co-cultured with Gel/Zr/EGCG1.0 hydrogel for two days (The nucleus is blue and the cytoskeleton is red). (C) Interacellular ROS scavenging capability of hydrogels evaluated by DCFH-DA (green fluorescence). (D) Statistics of fluorescence intensity for DCFH-DA (n= 4). (E) SOD level analysis results by H<sub>2</sub>O<sub>2</sub> stimulation (n= 4). (F) GSH/GSSG level analysis results by H<sub>2</sub>O<sub>2</sub> stimulation (n= 4). (G) MDA level analysis results by H<sub>2</sub>O<sub>2</sub> stimulation (n= 4).



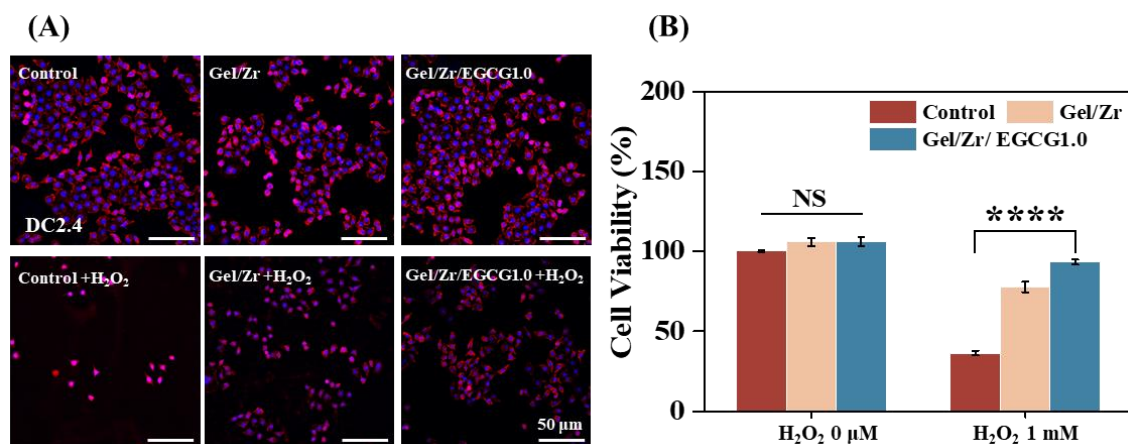


**Fig. S10. Viability and morphology of DC2.4 cells.** (A) Cytoskeletal structure of DC2.4 cells after incubation in the solution containing hydrogels and H<sub>2</sub>O<sub>2</sub>. (B) DC2.4 Cells survival rate measured by CCK8 kit after incubation in the solution containing hydrogels and H<sub>2</sub>O<sub>2</sub> (n = 3).

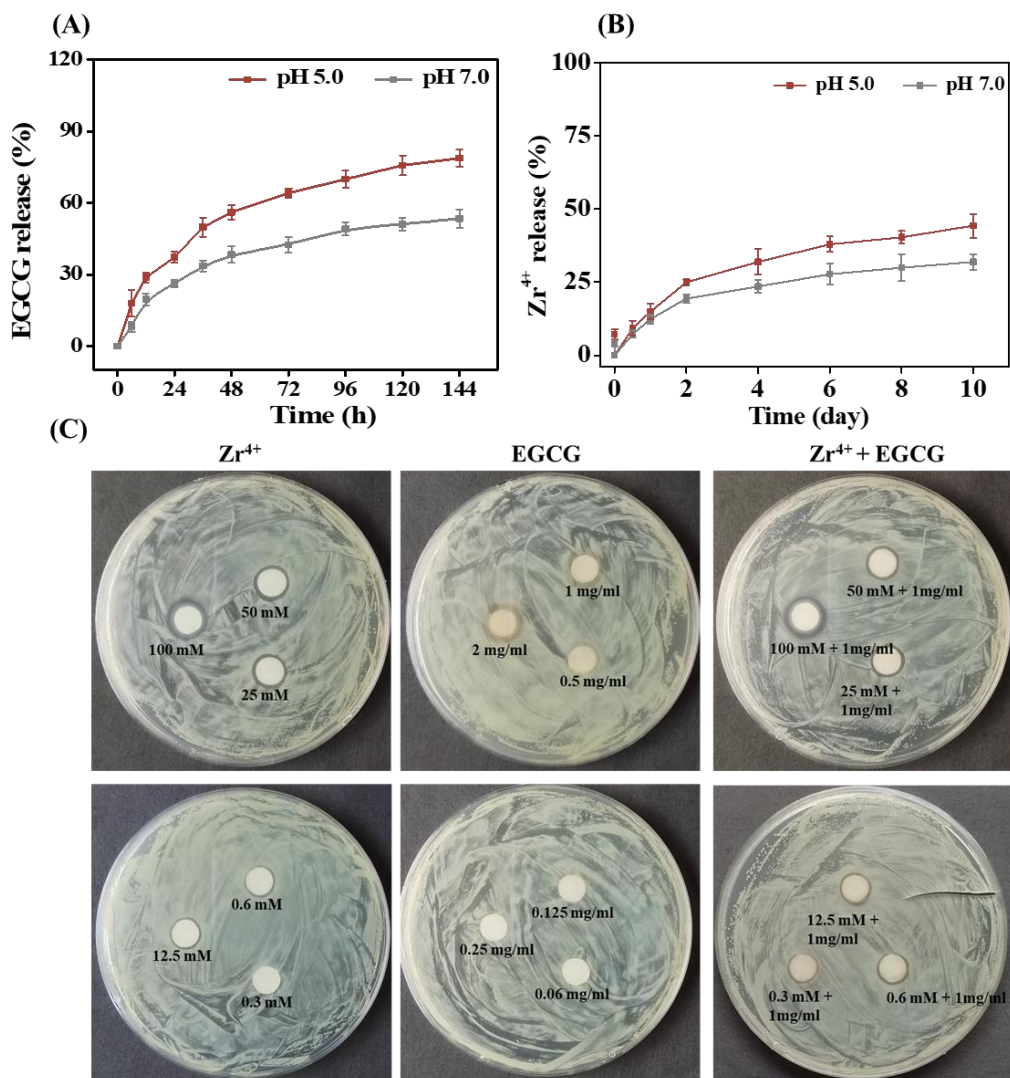


**Fig. S11. *In vitro* release experiments of EGCG and Zr from hydrogels, and the circle of inhibition of different concentrations of EGCG, Zr<sup>4+</sup>, and Zr<sup>4+</sup>/EGCG.** (A) EGCG release from Gel/Zr/EGCG1.0 hydrogels at different pH conditions (n = 3). (B) Zr<sup>4+</sup> release from Gel/Zr/EGCG1.0 hydrogels at different pH conditions (n = 3). (C) antibacterial sensitivity with agar diffusion test. A digital camera was used to collect images of the Zr<sup>4+</sup>, EGCG, Zr<sup>4+</sup>/EGCG samples different concentrations of *Staphylococcus aureus*. Summarized data showed the difference in inhibition zone diameters for *Staphylococcus aureus* among the different groups.

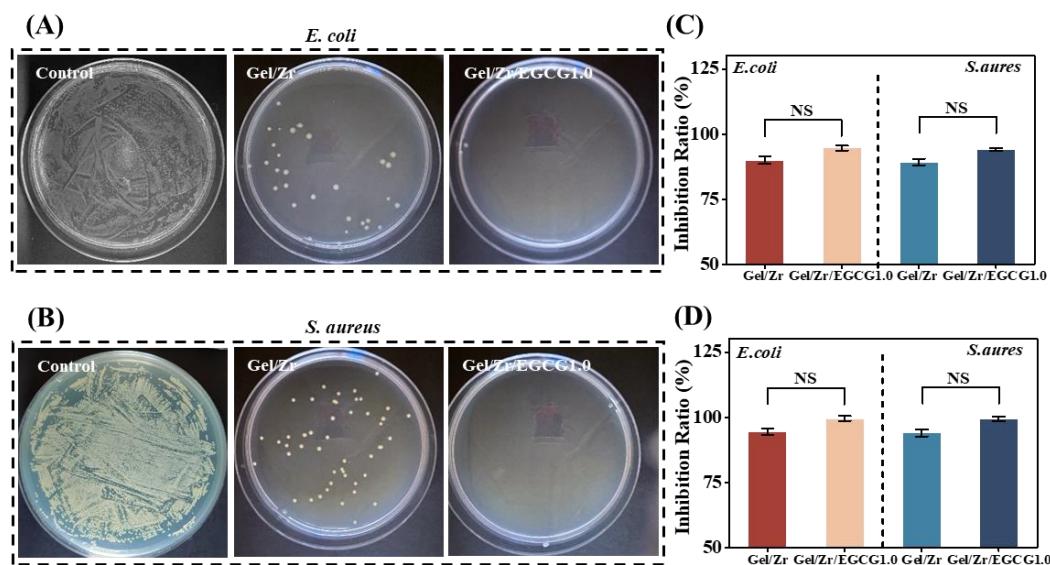


**Fig. S12. *In vitro* antibacterial test.** (A) *E. coli* survival diagram and (B) *S. aureus* survival diagram. (C) Histogram of the number of colonies on an agar plate. (D) The bacteriostasis rate of the indicated hydrogel at OD<sub>600</sub> nm was *E. coli* and *S. aureus* (n = 3).

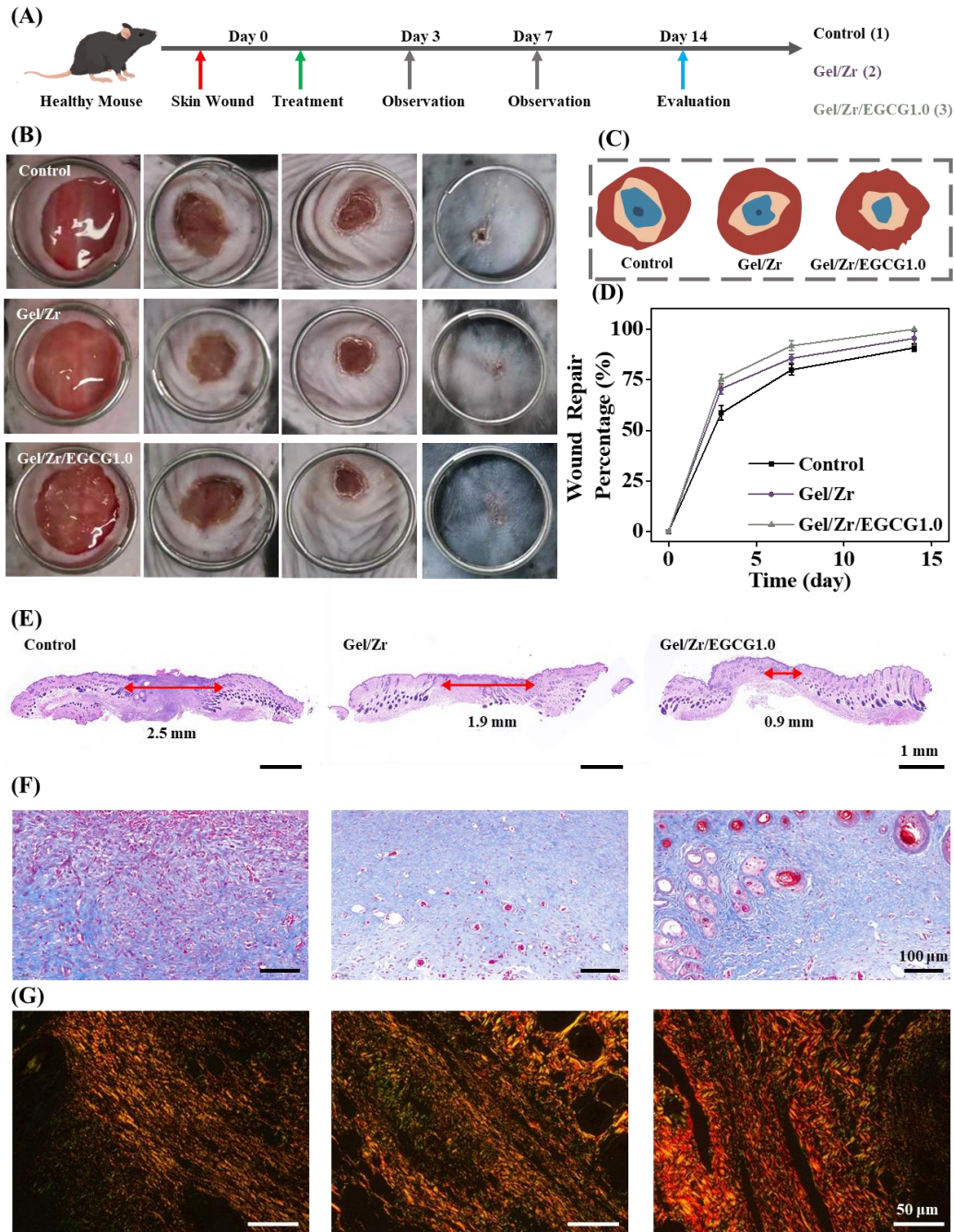


**Fig. S13. Wound healing and histopathological images of wound tissue in the healthy mice.** (A) Schematic illustration for acute wound generation and the subsequent healing process. (B) Representative photographs of acute wound healing on days 0, 3, 7, and 14. (C) Wound fractions healed by different treatments on days 0, 3, 7, and 14 (n = 3). (D) Quantitative analysis of wound area in each group (n = 3). (E) H&E staining of the wound area on day 14 (n = 3). (F) Partially enlarged Masson images. (G) Representative scarlet staining sections PS red (n = 3).

**Table S1.**

**Hydrogels are formed or not after different metal ions are mixed with 5% and 10% Gel after dissolving in an aqueous solution.** “No” means hydrogels cannot be formed, and “Yes” means hydrogels can be formed.

Metal ions	Concentration (mM)	Gelatin concentration ( Wt%)	
		5	10
<b>Zn<sup>2+</sup></b>	50	No	No
<b>Ag<sup>3+</sup></b>	50	No	No
<b>Ce<sup>3+</sup></b>	50	No	No
<b>Co<sup>2+</sup></b>	50	No	No
<b>Ca<sup>2+</sup></b>	50	No	No